Theor Appl Climatol (2013) 111:497–511
DOI 10.1007/s00704-012-0668-0

ORIGINAL PAPER

Urban climate and clues of heat island events in the metropolitan area of Rio de Janeiro

Andrews José de Lucena · Otto Corrêa Rotunno Filho · José Ricardo de Almeida França · Leonardo de Faria Peres · Luciano Nóbrega Rodrigues Xavier

Received: 24 July 2011 / Accepted: 2 May 2012 / Published online: 2 June 2012

Abstract This paper aims to map the thermal field in the metropolitan region of Rio de Janeiro (MARJ) considering the atmospheric characteristics and the land use that contribute to understanding the urban heat island. Three thermal maps are defined through the use of Landsat5-TM satellite images for three winter events chosen for the decades of 1980, 1990, and 2000, respectively. The results reveal a concentration of warmer cores in urban central areas as well as some local warmer areas in suburban region. Sites with lower temperatures correspond to vegetated areas which are away from the central part of the MARJ, including points of suburban areas. This work emphasizes the importance of the combined analysis of surface temperature with land use and atmospheric conditions, depicting a distinct pattern of heat islands for tropical climate.

A. J. Lucena (✉) · O. C. Rotunno Filho · L. N. R. Xavier
Laboratório de Recursos Hídricos e Meio Ambiente,
Programa de Engenharia Civil, Instituto Alberto Luiz
Coimbra de Pós-Graduação e Pesquisa em Engenharia,
Universidade Federal do Rio de Janeiro,
Caixa Postal 68540, 21945-970 Rio de Janeiro, RJ, Brazil
e-mail: lucenageo@yahoo.com.br

O. C. Rotunno Filho
e-mail: otto@coc.ufrj.br

J. R. A. França · L. F. Peres
Departamento de Meteorologia, Instituto de Geociências (IGEO),
Universidade Federal do Rio de Janeiro,
Av. Athos da Silveira Ramos, 274, CCMN (Bloco G),
Campus Ilha do Fundão—Cidade Universitária,
21949-900 Rio de Janeiro, RJ, Brazil

J. R. A. França
e-mail: jricardo@lma.ufrj.br

L. F. Peres
e-mail: leonardo.peres@igeo.ufrj.br

L. N. R. Xavier
Centro de Pesquisa em Energia Elétrica (CEPEL),
Avenida Horácio de Macedo, 354.,
Cidade Universitária,
21941-911 Rio de Janeiro, RJ, Brazil
e-mail: lnrxavier@gmail.com

A. J. Lucena
Departamento de Geociências, Instituto de Agronomia,
Universidade Federal Rural do Rio de Janeiro,
BR-465, Km 7,
23890-000 Seropédica, RJ, Brazil

1 Introduction

The urban climate highlights a complex environmental framework, which is attached in such a unique way to the city, a place of profound changes in atmospheric parameters, namely, in circulation, turbulence, and dispersion of air; in the albedo; and in the storage of heat due to evaporation and energy balance at surface (Taha 1997; Arnfield 2003; Kanda 2006). The heat island is the main product of the manifestation of urban climate and one of the important environmental problems of the twenty-first century (Rizwan et al. 2008). The expression heat island, well-known in the literature, was used for the first time by Manley (1958).

The heat island is so named because the spatial pattern of the isotherm forms one or more features called islands. The urban heat island (UHI) is formed by excess heat produced in urban areas, compared with the heat generated in their surroundings, generally undeveloped. In principle, the heat island refers to the increase in air temperature, but can also refer to the relative warmth of the surface. Thus, the heat island is a measure of difference (Voogt 2002) and does not refer to an absolute measure of temperature.

The heat island is characterized by three main aspects: its shape and configuration, its intensity, and location of its core warmer. These characteristics may define different configurations in each city, according to chronological time, as the time of day and season, to the weather from the prevailing weather situation, to geographical location, including its natural morphology, such as hills, water bodies, and green areas, and the shape and thermal properties of the materials that comprise the urban area.

The diurnal and seasonal variability are two other important factors. The most favorable periods for the manifestation of heat island can be detected and contrasted along the daytime, which take place in the hours of maximum diurnal heating or still of cooling at the time of night (Sun et al. 2009). Seasonally, sometimes in the summer and sometimes in the winter, different weather systems work for determining drier conditions, which usually are marked by more intense heat islands, or more wet conditions, usually marked by milder heat islands (Roth 2007).

The spatial pattern is influenced locally by surface characteristics such as parks, water bodies, and thickening of the built environment. For instance, the presence of a coast or valley in the topography of the city can add complexity to the UHI spatial characteristics because topographic effects, such as sea breezes, interact with the urban effects.

Just as the spatial variability, the heat island presents also a temporal variability along the day, which occurs as a result of differences in cooling rates between urban and rural areas. These differences occur due to the urban surface, weather conditions, or even the annual seasonality.

The intensity of the heat island was linked to the size of its population, as suggested by the early work of Oke and Maxwel (1967) and Oke (1982). In this case, a straight logarithmic relationship signals that most populous cities favor an increased intensity of the heat island, most common in the cities of Europe and North America. This fact leads to the conclusion that a most populous city has higher levels of urbanization in theory. In the work of Pongracz et al. (2006) applied to Budapest, one of the most populous cities of Hungary, the authors acknowledge a positive correlation of the intensity of heat island with its demography.

However, the circumstances favorable for the development of a heat island are characterized by a relatively high concentration of heat sources in cities (Oke 1982, 1987; Oke et al. 1991). The thermal properties of construction materials also facilitate the conduction of heat faster than soil and vegetation in rural areas, contributing to an increase in temperature contrast. The heat loss at night by infrared radiation into the atmosphere and into space in cities is partially offset by the release of heat from anthropogenic sources such as vehicles, industries, general construction, and construction materials that are relatively dense.

In town, the evapotranspiration rate, typically lower, further accentuates the temperature contrast with its surroundings. The drainage system (culverts) quickly removes most of the rain water so that only a small amount of radiation absorbed is used for evaporation (latent heat) and most of this radiation is used to heat the land surface and air directly (sensible heat). On the other hand, the wet surfaces of the rural areas (lakes, streams, soil, and vegetation) increase the fraction of absorbed radiation that is used for evaporation (Bretz et al. 1998; Taha 1997; Arnfield 2003).

The knowledge of the operation of the planetary boundary layer (PBL) is fundamental to understanding the spatial and temporal heat island (Grimmond 2006). PBL is a region of the atmosphere near the surface where turbulence is the dominant feature. It is affected by the surface on a time scale less than an hour and a vertical scale up to 2 km. The intensity of turbulence determines the spatial distribution of dynamic and thermodynamic properties and their vertical extent. Over continental areas, the turbulence is maintained by the wind throughout the day, intensified by thermal convection, and contained by the surface inversion layer at night. Its vertical extent ranges from 300–1,500 m during the day to 100–300 m at night (Oke 1976, 1997).

Another layer, the so-called urban boundary layer (UBL), extends above the roof level with characteristics produced by the urban nature of the surface, whose roughness, provided by the presence of relatively high buildings, causes a particularly aerodynamic. The wind speed is reduced, but there is an increase of turbulence and drag produced by air friction. The intra-urban layer or canopy layer (UCL) is a portion of the UBL stratified below the level of the roofs, which is produced by micro-scale processes on streets, among buildings (Oke 1997; Grimmond 2006).

A product generated or identified at the UCL is the urban canyons including the walls of buildings that create corridors among tall and concentrated buildings separated by streets. For such formation of urban canyons, a relationship between the dimensions height, width and length of urban construction, and the thermal properties of the material used (soil cover, building materials, among others) should be developed. Inside the canyon, the radiation undergoes multiple reflections between the streets and walls of buildings with different absorptions (Oke 1981, 1987; Grimmond 2006).

The effects of heat islands are diverse and largely negative, with implications for comfort and to human health (Voogt and Oke 2003), with direct and indirect environmental impacts by encouraging increased consumption of energy for cooling, which creates a footprint of high environmental cost (Stathopoulou and Cartalis 2007). The literature is significant in the last 20 years and it has been based on contributions in the methodologies and techniques employed (Arnfield 2003; Kanda 2006), from more traditional approaches such as studies of climatological time series with different statistical analysis

(Chung et al. 2004; Fujibe 2009; Homar et al. 2010) and the use of transects of fixed and mobile networks throughout the city (Sun et al. 2009; Murphy et al. 2011), to the latest procedures, such as remote sensing (Streutker 2003; Cheval et al. 2009; Stathopoulou and Cartalis 2007; Imhoff et al. 2010) and atmospheric modeling (Yoshikado 1994; Ezber et al. 2007; Van Weverberg et al. 2007; Karam et al. 2010; Oleson et al. 2011; Zhang et al. 2010), that have been treated with some frequency in conjunction with traditional methods to a more integrated analysis to detect the formation of heat islands.

We also observe that the scientific literature investigates the question of the formation of heat islands through analysis conducted for various towns and cities in the world, among which include Buenos Aires (Bejarán and Camilloni 2003), Beijing (Li et al. 2004), New Jersey (Rosenzweig et al. 2005), Hong Kong (Giridharan et al. 2007), London (Kolokotroni and Giridharan 2008), Tel-Aviv (Saaroni et al. 2000), Lisbon (Alcoforado and Andrade 2006), Bucharest (Cheval and Dumitrescu 2008), and Fez (Johansson 2006), among others.

Different studies have emphasized the role of land use in generating urban environmental anomalies for the city of Rio de Janeiro and its metropolitan area. For example, Rosa-Freitas et al. (2010) analyzed the heterogeneous space of the city and incidence of dengue cases. Heterogeneity was defined from the classification of urban ecosystems with the overlay of land cover maps of neighborhoods. The results show that these ecosystems are subject to different incidences of dengue. It should be highlighted the high rates identified in the lowland ecosystem of Jacarepaguá, which encloses an area characterized by the transition from an old rural area, still containing large vegetated areas, to an area of high rates of urbanization.

Marques Filho et al. (2009) highlight the importance of studies of urban climatology in tropical countries which appear quite different from temperate climates. The authors present some results of thermodynamics and UHI temporal evolution for the metropolitan area of Rio de Janeiro. Three groups of different microclimates were identified in the metropolitan region of Rio de Janeiro (MARJ). A behavioral pattern of the UHI can be determined by the temporal evolution of the differences between the virtual potential temperature in urbanized and vegetated areas, including the effects of moisture on the positive buoyancy of air parcels during the convective period. Another finding by the authors is that the tropical UHI in the MARJ occurs during the morning and not during the night, as in temperate areas. The UHI has a maximum daylight in the morning for all seasons, being more intense along the months in the transition between the rainy summer and dry winter (February–May) with an amplitude of 4–5 °C (as opposed to a range of 2–3 °C in the other months). Unlike what happens in the morning, late afternoon, and early evening, the difference is negative, indicating that the area with vegetation is warmer than the urban area. The minimum adverse occurs around 18:00 hours. The consequence of this particular phenomenon is the weakness of the wind (breeze urban) over the urban area.

Karam et al. (2010) simulate the occurrence of daytime heat island in MARJ during 2007 through the tropical town energy budget (t-TEB) scheme and compares with the observed data. The simulation t-TEB is consistent with climatological observations and supports the occurrence of daytime heat island. It appears that the time and the dynamics of UHI in tropical cities may vary significantly from the patterns observed in mid-latitude cities where the peak intensity of the heat island occurs in the morning and not at night. The causes for the occurrence of the UHI in the MARJ are mainly due to large influx of solar radiation used for heating of urban surfaces. In addition, there is the presence of vegetated areas on the periphery, increasing evapotranspiration, which occurs in association with the restored strength of the surface temperature.

This study encourages the inclusion of the city of Rio de Janeiro and its metropolitan area (MARJ) in the metropolitan network of monitoring the global urban atmosphere and offers an opportunity to disseminate information applied to tropical regions, relevant in the context of international urban climate studies. The site, the urban morphology, and atmospheric circulation have unique aspects that deserve to be evaluated and better understood. There is still a need to map their environment from the perspective of urban climatology.

Additionally, given the natural landscape of a tropical country, interspersed between hills, with emphasis on the presence of the valleys and forests and the nearby sea, the need for studies on environmental vulnerability is highlighted. Some aspects of this vulnerability include mass movements, flooding, air pollution, water resource availability in terms of quantity and quality, coverage and change in land use and, in particular, increase in temperature regimes, to the extent that urban regions occupy growing areas in cities, often in a disorderly way and without adequate urban planning.

The socioenvironmental framework outlined suggests a systematic study of urban climate in the MARJ to ensure conditions to manage and plan the space towards urban sustainability. Thus, the objective is to map the thermal field in the MARJ through remote sensing techniques and to identify areas potentially suitable for expression of the heat island and the corresponding factors responsible for its formation and by their spatiotemporal dynamics. The analysis is done from Landsat5-TM scenes, which were acquired for three dates, representative of the last three decades.

The paper contributes to the analysis of the phenomenon of formation of heat islands. First, by assuming that the absolute value of temperature obtained by the Landsat thermal image does not represent the value of the heat island, for in the benchmark adopted here means that the heat island should be measured from the comparison of differences between

temperatures and not from absolute values. Thus, the value of surface temperature obtained by remote sensing serves as an indicator to locate areas favorable to the heat island. Secondly, it leads to an analysis by the use of thermal images for better understanding of the spatial distribution of thermal field.

2 Study area

The MARJ is one of eight government regions of the state of Rio de Janeiro, located in southeastern Brazil and with the coast bathed by the Atlantic Ocean, including 19 cities: Rio de Janeiro, Belford Roxo, Duque de Caxias, Guapimirim Itaboraí Japeri, Mage, Nilópolis, Niterói, Nova Iguaçu, Paracambi, Burnley, São Gonçalo, São João de Meriti, Seropédica, Mosque, Tanguá, Itaguaí, and Maricá (Fig. 1).

By its geographical position and because of historical, economical, legal, and political processes, the MARJ is now the second largest concentration of population and economic activities in the country, containing a large volume of activities and work flows, a provision of more specialized goods and services, and a high rate of urbanization. In the state of Rio de Janeiro, the MARJ hosts on average 90 % of state population and it concentrates much of the regional services.

The urban set up in the MARJ, throughout its history of occupation and expansion, especially from the 1970s of the twentieth century, drew on in a splayed shape, with nucleus in the central city of Rio de Janeiro, showing the formation of branches that spread throughout the city, constituting the so-called growth vectors or occupation.

Physical space is marked by two distinct geomorphological units: the rocky mountains and the lowlands, scene of intense changes, shaped by human social work. The lowlands and the rocky mountains represented a major challenge to urban growth since the beginning of the occupation history with the establishment of a tough fight of man in front of natural obstacles. The social changes throughout history in the geographical space of the MARJ have resulted in a series of changes in the environmental system, reaching the water resources and pedologic, geomorphologic, biogeographic, and atmospheric systems.

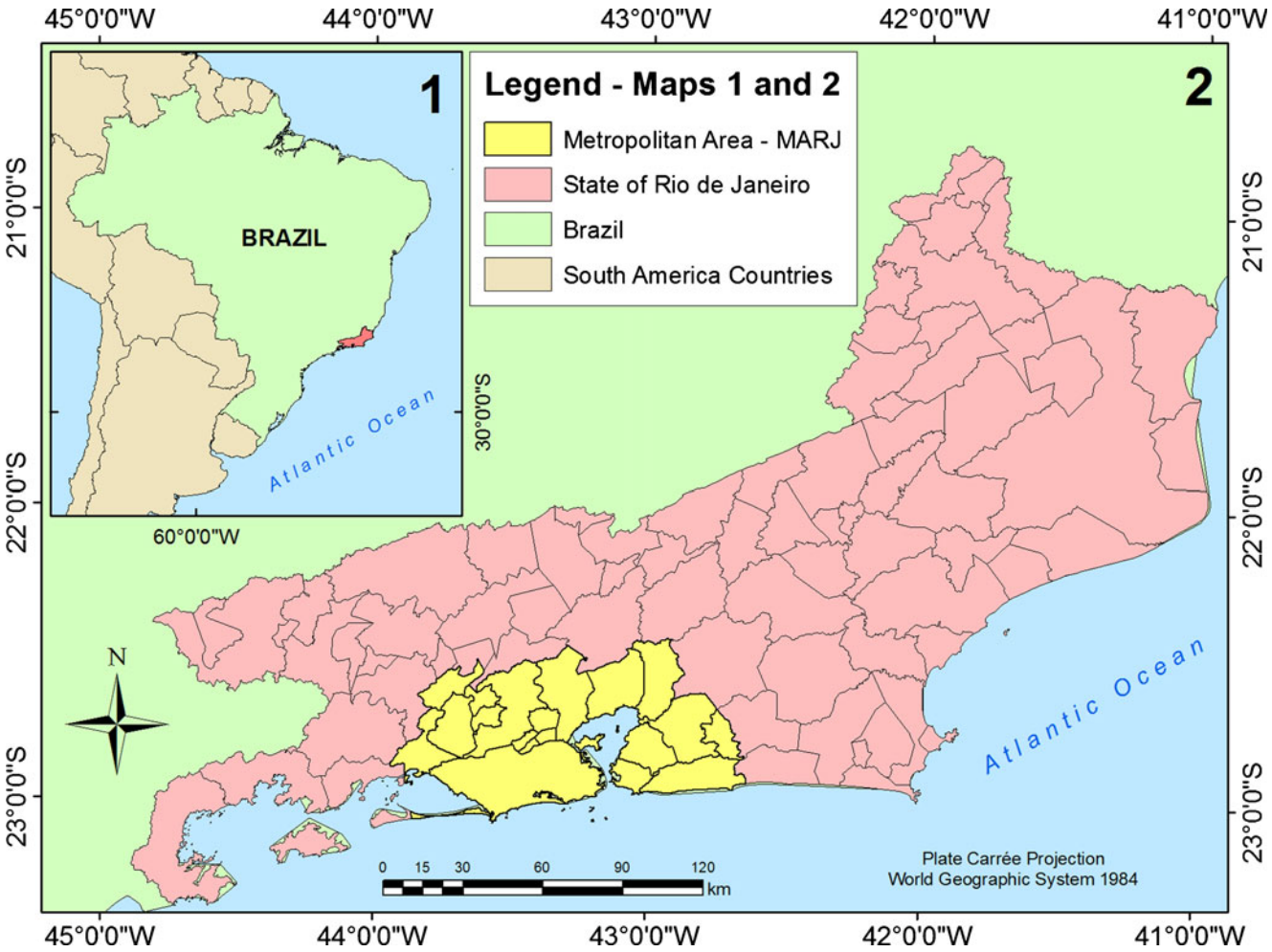

Fig. 1 Delimitation of the Metropolitan Area of Rio de Janeiro (MARJ) and its geographical location in Brazil and South America

3 Materials and methods

The use of remotely sensed images is an objective method for the assessment of urban heat islands (Gallo et al. 1995) and therefore an effective tool in urban climate studies through the use of thermal bands of sensors installed onboard of TIROS, NOAA, Landsat, and more recently onboard of Terra and Acqua.

Rao (1972) was possibly the first researcher to demonstrate the successful application of remote sensing in the study of urban climate. Using the thermal band (10.2–12.5 μm) of the satellite TIROS (ITOS-I), the author examined the surface temperature of cities throughout the mid-Atlantic coast. The Landsat3-MSS, Landsat5-TM, and Landsat7-ETM+ have been widely used for the temporal–spatial analysis of the climate of cities since the Landsat series present a remarkable acquisition period of time (Stathopoulou and Cartalis 2007; Yuan and Bauer 2007).

In this work, maps were drawn for soil use and occupation. In addition, maps and graphics with thermal transects along the MARJ were developed based on images from the sensor Landsat5-TM corresponding to point_217 and orbit_76, scene which covers the area of the MARJ. All digital image processing was developed using SPRING version 4.3, which is a computer code processing system of georeferenced and satellite information developed by INPE-Brazil.

We selected three dates for the production of maps and transects, namely 11/08/87, 25/08/1998, and 08/02/2007, for the austral winter periods. The local time of satellite pass occurs exactly at 0917, 0930, and 0942 hours, respectively. In general, except when cold front incursions cause instability, winter in southeastern Brazil records regularly, clear sky, cloudless and calm weather, and stable conditions favored by the South Atlantic anticyclone activity. The situations of atmospheric stability are extremely favorable for the heat islands occurrence, because the clarity and calmness favors the incidence of solar radiation reaching equally the entire region allowing also a better comparison between urban and rural areas. During the summer, such conditions are not always possible to occur due to cloud concentration that is favored by thermal lifting and the highly irregular geomorphology of the metropolitan area. It is noticeable that the winters in southeastern Brazil are not as stringent as in temperate regions and in southern Brazil. On the other hand, there are winter days with high daily temperatures well above 25 °C.

All images were georeferenced using the polynomial model first degree and nearest neighbor interpolation. Images Geocover_2003 composed of data from Landsat series (MSS, TM, and ETM+) were the basis for georeferencing.

The land use map was made for the three previously mentioned dates, highlighting the use and occupation of land in the MARJ, more specifically for the years 1980, 1990, and 2000. The classification of land use map was produced using the methodological approach of classifiers by regions or classification of segmented images, which, besides using the spectral information of each pixel, maintains the spatial information that involves the relationship between pixels and their neighbors. The classification procedure recognizes the homogeneous areas of images, based on spatial and spectral properties. The edge information is used initially to separate regions jointly with the spatial and spectral properties that will unite the areas with the same texture.

The supervised classification procedure used the distance measurement of Battacharya, which measures the statistical separability between a pair of spectral classes, i.e., it measures the average distance between the probability distributions of spectral classes. One advantage of this classifier is the user interaction, through training, which samples will be formed from the regions obtained in the image segmentation (Mather 1993). At the end of the processing, the four classes considered most relevant for analysis were extracted: urban, rural or urban with low density, vegetation, and water bodies.

Thermal maps were made based on the land surface temperature (LST) retrieval from remote sensing data. Although the use of satellite measurements appears to be very attractive, the radiance measured is affected by surface parameters, namely, temperature and emissivity, as well as by the thermal structure and composition of the atmosphere. Therefore, an accurate retrieval of LST from space data requires a proper characterization of the atmosphere influence (e.g., absorption and emission processes) as well as an adequate knowledge of LSE because natural surface does not act as blackbodies (Peres and DaCamara 2006; Peres et al. 2008). Accordingly, the temperature was obtained in this work by combining algorithms that take into account the atmospheric and emissivity effects on the signal registered at the top of the atmosphere by computing the atmospheric transmittance, the air temperature, and the land surface emissivity. Thus, the temperature here is referred to as land surface temperature.

Different studies have used the brightness temperature, which physically corresponds to the radiance at the top of the atmosphere without any atmospheric and emissivity correction, in order to analyze the UHI phenomenon. However, its is worth noting that the brightness temperature may be quite different to the actual temperature of the surface (Weng et al. 2004; Zhang et al. 2009; Jiang and Tian 2010; Peres et al. 2010). The work of Sobrino et al. (2004) shows progress with the inclusion of the atmospheric correction in the calculation of surface temperature. Lucena et al. (2010b) compared the temperature obtained without atmospheric correction (brightness temperature) to the temperature determined using atmospheric and emissivity correction (land surface temperature) for MARJ in Rio de Janeiro and the differences can reach up to 20 °C depending on the atmospheric and surface conditions.

In this work, LST maps were developed based on Landsat satellite data. In order to obtain LST values, raw data in digital

numbers (DN) were first converted to radiance as follows (Chander et al. 2009):

$$L_i = \left(\frac{\mathrm{LMAX}_i - \mathrm{LMIN}_i}{\mathrm{Qcal}_{\max}}\right)\mathrm{Qcal} + \mathrm{LMIN}_i \quad (1)$$

where L_i is the spectral radiance in band i in watts per square meter per steradian·per·micrometer; LMAX_i is the value of the band maximum radiance in band i in watts per square meter per steradian·per·micrometer ; LMAX_i is the value of the minimum radiance in band i in watts per square meter per steradian·per·micrometer; Qcal is the value of DN; and $\mathrm{Qcal}_{\max}$ is the maximum value of DN, which is equivalent to 255 for all bands. The values of LMAX_i and LMIN_i for each Landsat band may be obtained in Chander et al. (2009).

After the conversion of DN in radiance, brightness temperature values in Landsat infrared band 6 were computed based on the inversion of Planck function

$$T_\mathrm{b} = \frac{K_2}{\ln\left(\frac{K_1}{L_i} + 1\right)} \quad (2)$$

where T_b is the brightness temperature in Kelvin, K_1 and K_2 are the Landsat calibration constants 1 and 2 in watts per square meter per steradian·per·micrometer, which are equal to 607.76 and 1,260.56, respectively.

The LST retrieval is performed based on Souza and Silva (2005) algorithm according to Eq. (3)

$$T_\mathrm{s} = T_\mathrm{b} + \Delta T \quad (3)$$

where T_s is LST in Kelvin, T_b is the brightness temperature in band 6 obtained according to Eq. (2), and ΔT is the correction factor to obtain the LST from the brightness temperature in band 6 given by

$$\Delta T = \frac{B_\mathrm{i}(T_\mathrm{b})\left(\frac{1}{\alpha_1} - 1\right) - \frac{\alpha_2}{\alpha_1}B_\mathrm{i}(T_\mathrm{a})}{\frac{\partial B_\mathrm{i}(T_\mathrm{b})}{\partial T_\mathrm{b}}} \quad (4)$$

Where B_i (T) is the Planck function on describing the radiance of a blackbody of temperature T in the unit of watts per square meter per steradian·per·micrometer; α_1 and α_2 are known as:

$$\alpha_1 = \tau_i \varepsilon_i \quad (5)$$

$$\alpha_2 = (1 - \tau_i)[1 + (1 - \varepsilon_i)\tau_i] \quad (6)$$

It is worth noting that the correction factor ΔT takes into account both the atmospheric and emissivity influence in the signal recorded by the instrument on board the satellite. Accordingly, in order to retrieval LST based on Eqs. (3)–(6) it is necessary to know the different atmospheric parameters, namely, atmospheric transmittance τ_i, effective mean atmospheric layer temperature T_a, and also the land surface emissivity ε_i. For instance, T_a was obtained according to Qin et al. (2001) as follows

$$T_\mathrm{a} = 19.73 + 0.909T_0 \quad (7)$$

where T_0 is the air temperature at 2 m. The atmospheric transmittance τ_i was computed based on an empirical relationship obtained by Souza and Silva (2005) that uses the water vapor content w in gram per square centimeter as input

$$\tau = 0.951 - 0.01 \cdot w \cdot \exp\left(\frac{3w}{1 + w}\right) \quad (8)$$

Values of water vapor were achieved based on the relative humidity and the saturation pressure of water vapor according to Leckner equation (Iqbal 1983). Accordingly, air temperature at 2 m and relative humidity data were obtained by the monthly average of all weather stations present in the MARJ. The MARJ has been divided into four sub-regions (west zone, lowland Bangu, central, and eastern section of the Guanabara Bay), and then, an average initial value was estimated to each of the sub-regions. Next, we calculated an overall final average defined based on the initial average values corresponding to each of the four sub-regions.

Finally, the land surface emissivity is retrieved based on the Van de Griend and Owe (1993) algorithm, which relates emissivity and the vegetation index NDVI

$$\varepsilon_i = 1.009 + 0.047 \ln \mathrm{NDVI} \quad (9)$$

Accordingly, NDVI values were computed as follows (Huete et al. 2002):

$$\mathrm{NDVI} = \frac{\rho_4 - \rho_3}{\rho_4 + \rho_3} \quad (10)$$

where ρ_3 and ρ_4 are, respectively, the reflectance in bands 3 and 4, which are obtained based on the radiance L_i

$$\rho_i = \frac{\pi L_i d^2}{\mathrm{ESUN}_i \cos\theta_\mathrm{s}} \quad (11)$$

where ESUN_i is the average solar irradiance on channel i in watts per square meter per micrometer, whose value are 1,554 and 1,036 for bands 3 and 4, respectively, d is the Earth–Sun distance in astronomical units, and θ_s is the solar zenith angle.

The LST images, initially in Kelvin, were converted to degrees Celsius and then classified according to standard temperature ranges in order to establish a single criterion when comparing images. Finally, we adopted the parametric two-sample t test for difference of means under one-tailed hypothesis test (Wilks 2006). The method of hypothesis testing was conducted to compare the true mean LST for the classes of land use, "urban," "rural or urban low density," and "vegetation," for every decade analyzed in this work at the 99.9 % confidence level.

We chose to compare the classes per decade, and not between decades, because we understand that a single image per decade may be subject to intense current atmospheric interference of the state. Thus, comparison by decade will reveal the role of each class in the temperature, regardless of the weather situation instantly.

The null hypothesis formulated was that the mean LST for the urban class is equal to the mean of the other classes, while the alternate hypothesis is simply that the mean LST for the urban class is larger than the corresponding values for the other classes. Table 1 summarizes the LST sample statistics for the classes of land use. The results of the statistical test confirmed that the null hypothesis can be rejected at the level of 0.1 %, which means that we can assume that the average temperature for urban land surface is higher than the average LST values for the other classes of land use.

4 Analysis and results

4.1 The use and land cover for MARJ

The land use in the MARJ has a concentration of class "urban" in the west region of the Guanabara Bay, just in the marshland of Guanabara Bay, which stretches like a great spot for all around the edge of the Tijuca neighborhood and toward sector north and west of the map (Fig. 2). Another great spot of the class "urban" appears in the east region of Guanabara Bay, as well as enclaves or clusters identified in the extreme north and in areas to the northwest and west. In the following decades, there is a spreading and juxtaposition of the class "urban" in the directions east, west, and north of Guanabara Bay and around Pedra Branca and Mendanha hill (Figs. 3 and 4).

The class "urban low density" in the 1980s of the last century is predominant in the periphery of the class "urban," such as in north areas and east and west ends of the Guanabara Bay (Fig. 2). In the following decade (1990), this class is reduced, becoming more sparse, but still very homogeneous in the most east of the bay (Figs. 3 and 4).

The class "vegetation" is mainly concentrated in the lasting rocky mountains of the city of Rio de Janeiro (Tijuca, Pedra Branca, and Mendanha), in the foothills of the Sea mountains until their highest parts, which starts from the Sepetiba Bay in the west and extends into the interior part of the mountainous region. Another domain space of this class is the swamp area at the bottom and at the north of Guanabara Bay, where there is an Environmental Protection Area, and in the in the vicinity of coastal lagoons.

In flat areas, which consists of lowlands, there are green clusters in a very heterogeneous space; however, there has been a visually perceptible increase of the green spot in the northern portion of Guanabara Bay on a map of 2007, which can be associated with the Environmental Protection Area or even with extinct farmland that could have been misclassified as "vegetation."

The spatial pattern of land use classes of the MARJ in these three time periods (1987, 1998, 2007) obeys the vector of occupation and expansion of the urban spot in the MARJ, as discussed earlier. The graph in Fig. 7 shows the evolution of classes in the MARJ. Although slight, variation and evolution of land use classes show a mild increase in "urban" and "vegetation." The class "rural or urban low density" is the most significant in terms of involution and variability. This class presents a falling rate that is most pronounced between 1987 and 1998 and follows on decline in 2007. This class is the most complex to be defined in the segmentation for classification, as it is still a type of class that faces conflict over legalizing the occupation with the city government and, therefore, feasible to support the fact that this is the class that showed major changes.

Finally, comparing the average LST between the classes of land use (Table 1), which will be further discussed in the following section, the class "urban" in all years has the highest average, followed by the "rural or urban low density" and "vegetation." Once the statistical test for a confidence interval of 99.9 % (Table 1) has been applied, all changes revealed to be highly significant.

4.2 Thermal field conditions in winter and heat island scenarios

4.2.1 August 11, 1987

The LST varied spatially between 20 and 36 °C (Fig. 5), predominantly mean values of 29.8 °C for class "urban," 25.3 °C for class "vegetation," and 27.6 °C for class "rural

Table 1 LST values and standard deviation for the classes of land use in MARJ

Year	Class					
	Urban		Rural or urban low density		Vegetation	
	Mean	Standard deviation	Mean	Standard deviation	Mean	Standard deviation
1987	29.8	2.25	27.6	2.63	25.3	2.77
1998	36.5	2.65	34.1	2.89	31.8	2.82
2010	32.9	3.21	30.4	3.1	26.4	2.81

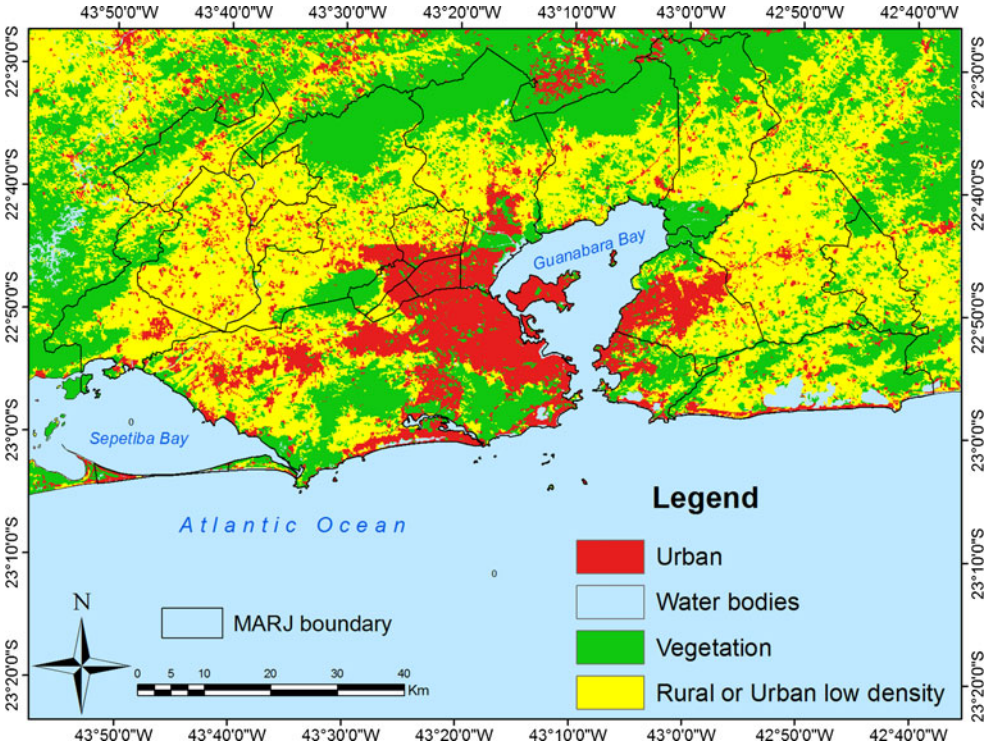

Fig. 2 Land use for Metropolitan Area of Rio de Janeiro (MARJ) in 1987

or urban low density" (Table 1). Among the "urban" and "vegetation," there is a difference of almost 5 °C. The hottest cores on the map, yellowish, above 30 °C, were located in Guanabara lowlands in the far west of MARJ and on the north side of the coastal range.

The southern coast, on the windward side of the massif of Pedra Branca, stands out with an extensive yellow bead with orange dots setting values above 34 °C. A similar phenomenon occurs east of the bay. Besides the yellow thread that involves the entire east coast, isolated hot enclaves above

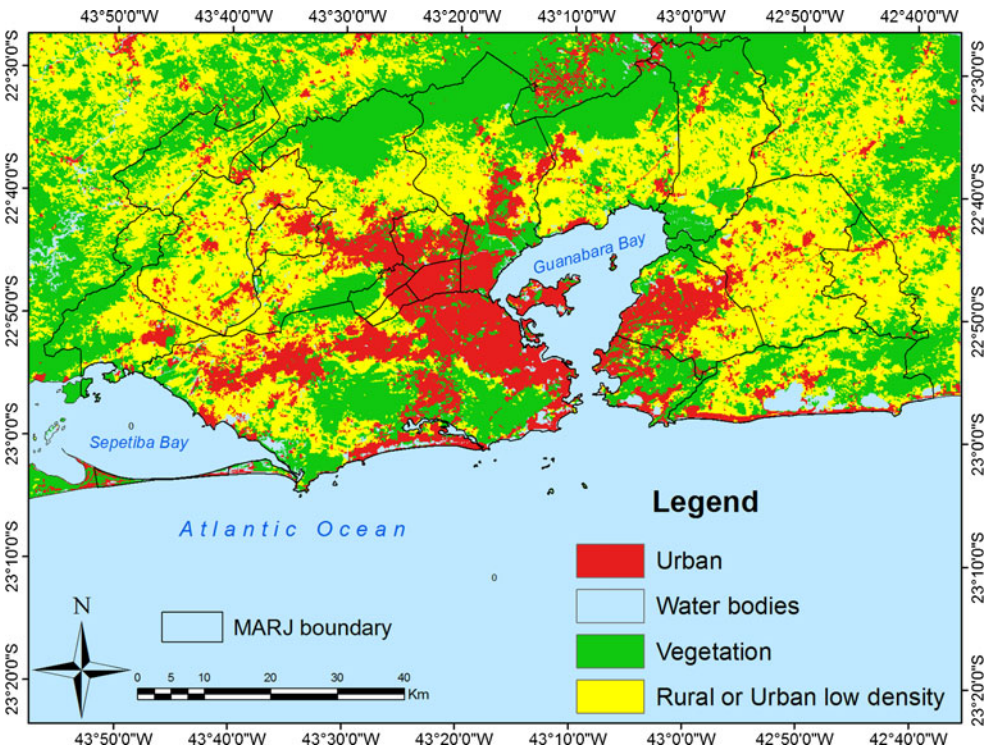

Fig. 3 Land use for Metropolitan Area of Rio de Janeiro (MARJ) in 1998

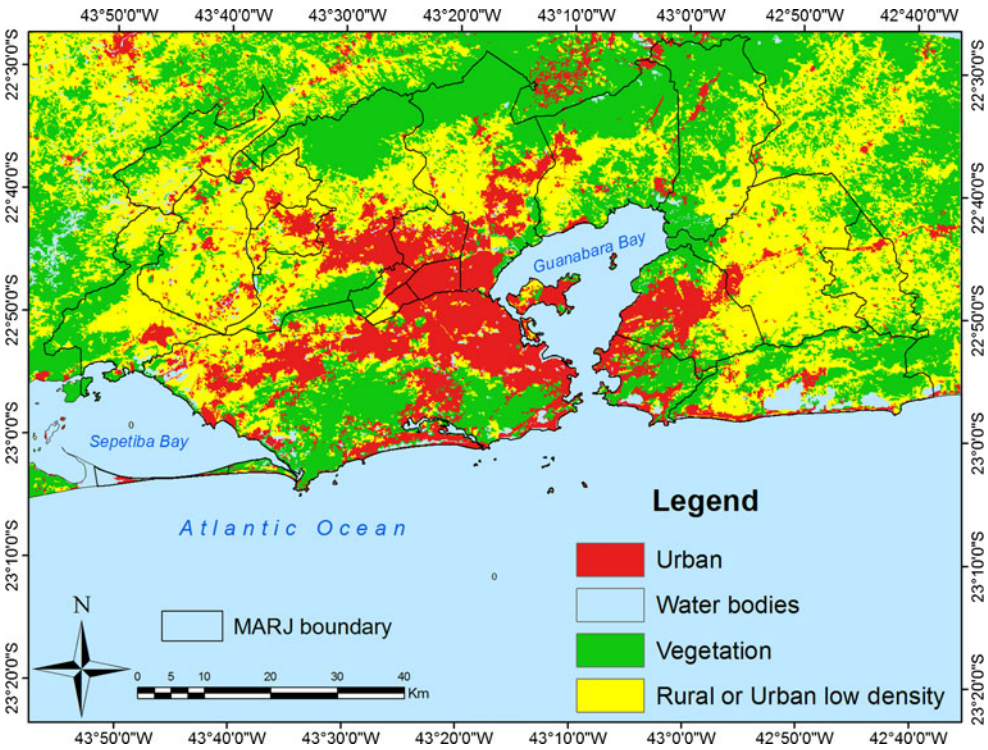

Fig. 4 Land use for Metropolitan Area of Rio de Janeiro (MARJ) in 2007

34 °C are identified in the cities of the east coast, spreading toward the eastern end (Fig. 5).

In the far west or northwest, a large yellow stain with values between 30 and 34 °C are located on the highest values of all MARJ, qualifying these areas as strongholds of the urban heat island. There is no direct relationship with the class "urban," because it is an area with predominant "rural or urban low density" or other uses, such as exposed soil not considered in the classification. The geographical situation of this region should be considered for a better understanding,

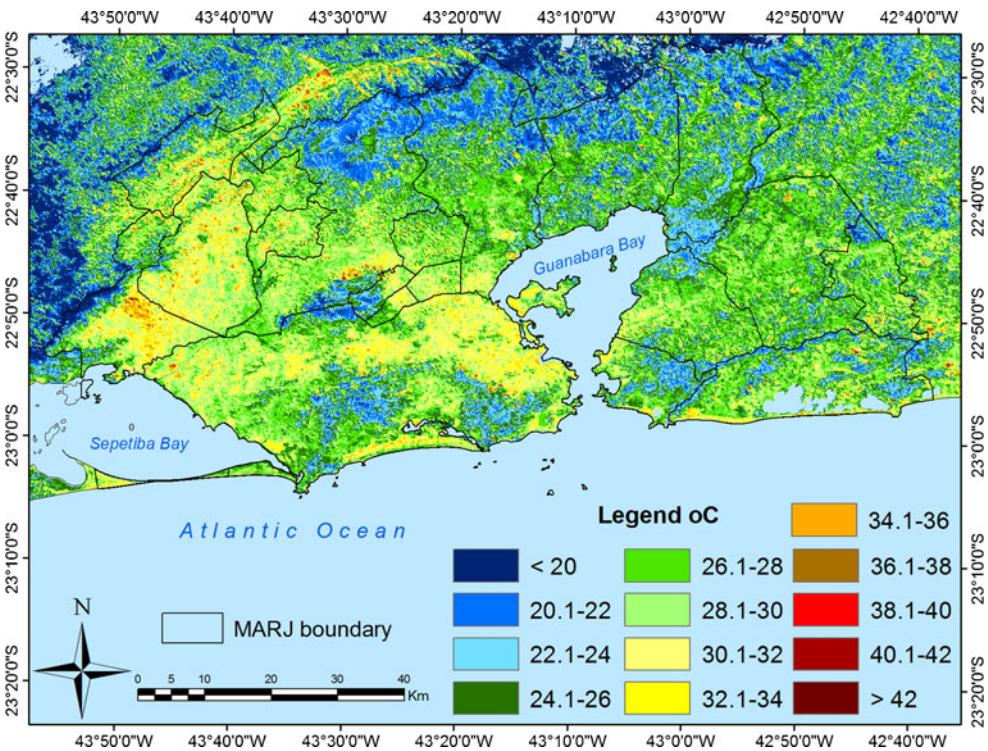

Fig. 5 Land surface temperature retrieval using Landsat-5 TM data for Metropolitan Area of Rio de Janeiro (MARJ) on August 11, 1987

because it is a large area of low and horizontal occupancy, in which the basal heating is extremely favored at this time in the morning when compared to a more coastal area.

There are also other noteworthy areas of the metropolis. The central region of the map, west of the Guanabara Bay, shows points in red (above 38 °C), which represent occupation areas along the slopes of the coastal range. Nonetheless, it should be emphasized that the coldest areas (below 24 °C) are situated in the three major metropolitan rocky mountains, in lighter blue, and also in the Serra dos Órgãos hill, located in the far north, in darker blue. This shows the role of these regions that despite the intense process of occupation of their slopes, vegetation in the MARJ and surroundings is still retained.

4.2.2 August 25, 1998

The thermal map of MARJ for 1998 has values much higher for the LST (Fig. 6) than 1987, ranging between 24 and 40 °C. The average temperature reaches 36.5 °C for "urban" class, 34.1 °C for the "rural or urban low density" class, and 31.8 °C for the "vegetation" class (Table 1). Therefore, similar to 1987, the difference between the two contrasting classes is about 5 °C. A gradation of colors from blue, with the lowest temperatures, to the darkest red, with higher temperatures, marks the thermal transition between the classes of land use, that is, between "vegetation" and "urban."

The spots in reddish and brown tones are concentrated in the east and west of the Guanabara Bay, which concentrates the bulk of the urban metropolis, and extends toward the far west and northwest, east, and northeast. Many of these areas are similar to those identified in August 1987 (Fig. 6), as in the far west, becoming potential spaces for expression of heat islands. Temperature values between 28 and 34 °C, in shades of green and yellow, appear in the large class "rural or urban low density," marking the transition characteristic as a class feature. Milder temperatures below 28 °C are located on the slopes of Serra do Mar mountains, in the northern section of the map, on the coastal massive mountains, in the surroundings of the coastal lagoons, and in the bottom of Guanabara Bay at its north part. Once more, the green mass of vegetation plays its role as thermal regulator inside MARJ.

4.2.3 August 26, 2010

The thermal map of the LST shows values between 26 and 38 °C for August 26, 2010. The average values are 32.9, 26.4, and 30.4 °C for "urban," "vegetation," and "rural or urban low density" classes, respectively (Table 1). The "urban" class is still the one that concentrates the highest temperature values, as opposed to "vegetation," with a gradient of 6.5 °C. The hottest nuclei of "urban" class in tones orange and dark orange are situated on the western shore of Guanabara Bay, extending toward extreme west and northwest. Warmer enclaves in red, above 38 °C, spread through different small areas, can be found in the east and west of

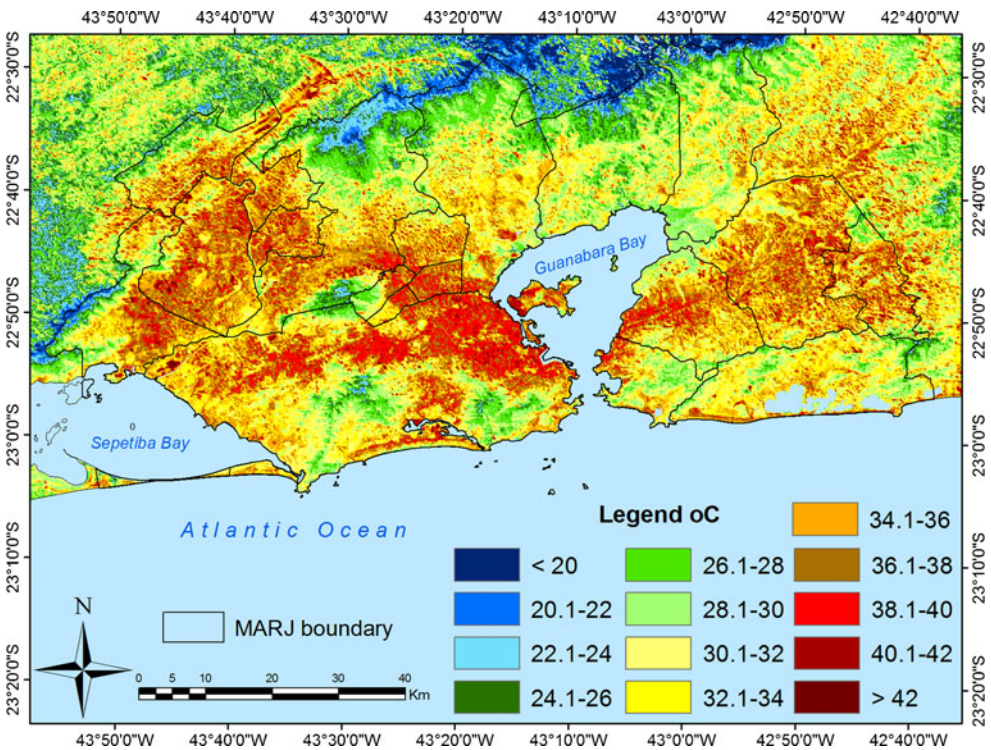

Fig. 6 Land surface temperature retrieval using Landsat-5 TM data for Metropolitan Area of Rio de Janeiro (MARJ) on August 25, 1998

Guanabara Bay, especially on the slopes of the massive mountains and counties in the far west (Fig. 7).

The cooler spots in tones yellow and green, between 26 and 34 °C, are located in the transition class between "urban" and "vegetation," more precisely in the "rural or urban low density" class, which surrounds and sometimes permeates the "urban" class. On the other hand, the lowest temperatures, in dark green and blue, less than 26 °C, are restricted to the cardinal edges of the map and to the coastal range.

5 Conclusions

The spatial distribution of the warmer and milder areas is quite similar in the three winter situations analyzed here, varying the thermal scale. We should be careful to not name these warmer areas as heat islands, but just as indications, considering that the heat island is a measure of difference, as stated in Voogt and Oke (2003). In this paper, we used the absolute temperature as an approach to identify the areas prone to concentration of heat. Furthermore, in future researh, the terminology heat island can be employed when calculating the relative and difference values based on absolute temperatures.

The analysis of thermal field by means of remote sensing is a reliable tool and deserves to be improved. The use of algorithms for atmospheric correction as used in this work is one of the possible improvements. In a previous study, as discussed by Lucena et al. (2010a), the atmospheric correction allows the representation of the actual temperature of land surface, as opposed to only the brightness temperature. For instance, the brightness temperature does not take into account the weather conditions, which can influence and lead to wrong values for the surface temperature. The authors found differences of over 10 °C for the corrected temperature in comparison to the brightness temperature.

In general, under conditions of atmospheric stability, with no clouds and no wind, the literature has shown that these are the ideal conditions to identify heat islands, especially at night (Voogt and Oke 2003). Under these conditions, the surface cools more quickly, thus making it possible to identify the areas most heated and cooled. Based on the images analyzed in this paper, under cloudless conditions, it was found that the temperature found for this scenario was indeed the highest, such as what occurred on August 25, 1998. Other variables should be jointly considered in further analysis to highlight and confirm this result, such as air humidity and insolation, fundamental elements of the atmosphere to better understand surface temperature.

The time of passage of the satellite must also be considered. In the case of Landsat images, its time of passage varies between 9:00 and 11:00 a.m. for the southern hemisphere, in a period that is already underway diurnal heating. In the case of the MARJ, which has a site interlaced between urban, forest, valleys, hills, and the sea, many meteorological variables, as wind, have a very particular behavior, which can

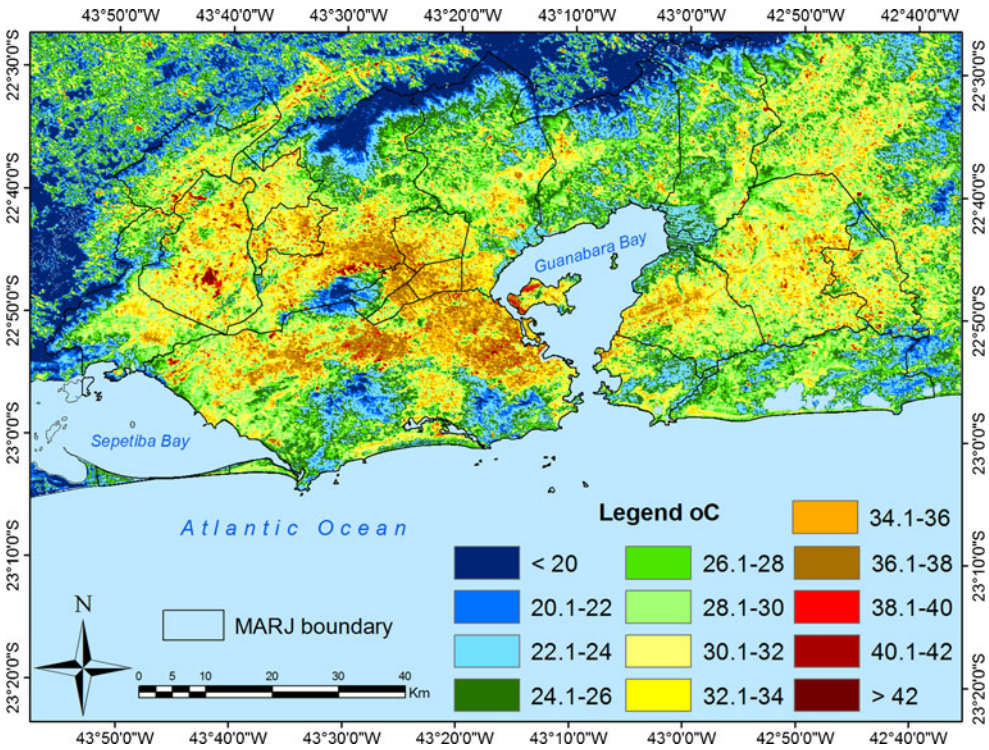

Fig. 7 Land surface temperature retrieval using Landsat-5 TM data for Metropolitan Area of Rio de Janeiro (MARJ) on August 26, 2010

influence the spatial distribution of temperature. For the wind, for example, mesoscale meteorological models may be used as a complementary tool to remote sensing technique, as they can simulate the wind directions to an area of rugged topography such as the MARJ identifying the main air flows entering the region.

Unique atmospheric models applied to urban areas are known from the work of Masson (2000), Lemonsu et al. (2004), and Pigeon et al. (2008). The use of modeling studies of heat islands became a wide spread practice more recently, as the reviews presented by Hafner and Kidder (1999) and Kanda (2006) adequately highlight. Therefore, mesoscale models such as RAMS and MM5 have been used to simulate the urban heat island (Lin et al. 2010; Kinouchi and Yoshitani 2001; Velazquez-Lozada et al. 2006). For a greater level of complexity of the urban surface, such as the UBL and the UCL, three-dimensional models have been applied as an alternative to estimate the surface energy balance within the urban canyons (Vukovich et al. 1976; Arnfield 1982; Oke 1987; Grimmond and Oke 1991; Grimmond and Oke 2002; Yoshikado 1992; Masson 2000; Kusaka et al. 2001; Martilli et al. 2002).

In this context, two works stand out for MARJ. The study conducted by Karam et al. (2010), previously mentioned in this paper, since it is an important reference with respect to the modeling approach in MARJ. In addition, Lucena et al. (2011) show that the hottest areas are prone to increased convective rainfall. This last analysis was based on the use of thermal images from the Landsat satellite and simulations of latent sensible heat, temperature, temperature advection, boundary layer height, air relative humidity, and wind speed and direction using the MM-5 model. Therefore, it is suggested that modeling be more frequently used in studies of heat island for MARJ where other elements of the climate, besides temperature, can be incorporated. Similar works with respect to the methodological modeling approach have been developed for other regions of Brazil (Karam et al. 1996; Oliveira et al. 2003; Carfan et al. 2007; Freitas et al. 2007).

Although the heat islands have not been established in this work, since it is a nomenclature that refers to the differences in temperature, it was possible to spatially delineate some heated areas, namely the western and eastern shores of Guanabara Bay, which correspond respectively to the lowlands of Guanabara and to the region of Niterói and São Gonçalo, as well as the southern edge of the track west of Guanabara Bay and enclaves distributed along Baixada Fluminense and west zone, which corresponds to the extreme northwest and west, respectively. On the other hand, the milder areas, which in future work could be named islands of freshness, are located in the proximity of the massive coastal covered with forest, around ponds and in the north coastal region of the Guanabara Bay.

Moreover, the statistical analysis evaluation for land use classes (Table 1) shows the role of urban temperature. In 3 years corresponding to three different decades, regardless of the absolute value of the LST, the class "urban" presented the highest average temperatures as opposed to "vegetation." However, areas of the class "rural or urban low density" also showed high values (not greater than or equal to "urban"), representing a transition area in the metropolis between rural and urban.

The inclusion of areas of the far east and west and northwest in the circuit of the most heated areas is subject of inquiry, as it represents not only the suburbs and the periphery, but also the suburban fringe, with land use classified as "urban low density." This result clearly defines the role of land use in the city as an important player in determining the corresponding temperatures. The multiple facets of the urban metropolitan space, featured by a dense urban use that blends with areas classified between the "almost urban" and the "old countryside," makes the "urban" attribute a very important information to consider, since it is part of the hypothesis that urban areas provide more favorable conditions for heating. One challenge is to identify other characteristics of the metropolitan soil use, without being exactly "urban," which promotes the accumulation of energy and therefore higher temperatures. For instance, it may be quite possible to incorporate the class "bare soil," with was not considered in this analysis. Bare soil could be related to rock outcrops, stretches of sand, or fallow land (or not occupied) that show a very similar spectral proximity to the category "urban" or "building area" in remotely sensed images as discussed by Zha et al. (2003).

Another issue that deserves to be raised is the role of the suburb of developing countries like Brazil, in the energy balance. The reality is quite different from that described by Arnfield (2003) with respect to the American suburbs, with well-spaced streets, parks, and wooded and airy presenting themselves as comfortable places. The suburb of MARJ goes against the American suburb or even the European suburb. Areas are uncomfortable, lacking adequate housing and sanitation, arid areas with little or no trees, overlooking a significant population who often live in unsanitary conditions, such as slums. It is therefore not surprising that these suburban areas register temperatures as higher or even larger than the central area, located east and west shores of Guanabara Bay, as was seen in winter thermal images of MARJ. The improvement of urban climate research in the MARJ might confirm this first clue and allow to establish a different framework for the configuration of urban temperature in tropical countries compared to that of temperate countries, as highlighted by Roth (2007).

This spatial distribution of the hottest nuclei in the metropolitan area should find greater accuracy from a more detailed analysis of land use and from the analysis of a larger number of available satellite images. In addition, it is important to select sensors that do the screening at other times besides the morning and to adopt higher spatial

resolution sensors and more thermal channels to precisely analyze and identify hotter areas. Also, it should be mentioned that the use of atmospheric models exclusive to urban areas are under development as presented in Masson (2000); Lemonsu et al. (2004); Pigeon et al. (2008), and Karam et al. (2010). However, there is still a need for further investigation of atmospheric models for providing simulations with higher spatial resolution, being able to recognize the properties of each type of land use and to determine the corresponding components of the energy balance.

The seasonal scenario which was examined in this paper deserves to be highlighted. We chose the austral winter, and especially for the month of August, due to the prevailing stability conditions. The winter of Rio de Janeiro is not very strict as in other parts of Brazil, which means that very high values of surface temperature can be detected under intense radiation, near 40 °C, as observed in 1998 and in 2010, and still in the mornings. Further comparisons with the temperatures along the summer should be conducted to analyze variations between both seasons.

This work represents the beginning of a systematic study of urban climate of the MARJ incorporating methodologies and approaches that can allow a deeper understanding of the climate dynamics of metropolitan areas of tropical cities of the southern hemisphere, which have distinct particularities and singularities when compared to other regions of the globe.

Acknowledgments The first author acknowledges the support provided by Fundação de Amparo à Pesquisa do Estado do Rio de Janeiro (FAPERJ) through a PhD scholarship granted to carry out this work. The authors would like to thank the Civil Engineering Program of Instituto Alberto Luiz Coimbra de Pos-Graduacao e Pesquisa de Engenharia (COPPE)—Universidade Federal do Rio de Janeiro (UFRJ) through the support of the Laboratory of Water Resources and Environmental Issues, the Department of Meteorology—Instituto de Geociências (IGEO)/UFRJ, and Instituto Nacional de Pesquisas Espaciais (INPE), with respect to data and infrastructure provided by these institutions for this research. The authors also recognize the support of Conselho Nacional de Desenvolvimento Científico e Tecnológico (CNPq), through the Programa Sul-Americano de Apoio às Atividades de Cooperação em Ciência e Tecnologia (PROSUL)—Process 490684/2007-6, which deals with remote sensing techniques applied to hydrological monitoring and climate change and the support of Secretaria de Educação Superior (SESu)—Ministério da Educação (MEC)—Coordenação de Aperfeiçoamento de Pessoal de Nível Superior (CAPES)—AUX-PE-PET-1228/2009 (PET CIVIL UFRJ), Project PEC/COPPE—FAPERJ 014/2010 (2010–2012), Project FAPERJ—Process E-26/103.116/2011 (2012–2014), Project IME-PEC/COPPE—CAPES—Aux-PE-PRO-Defense 1783/2008 (2008–2012), and MCT/FINEP/CT-HIDRO—Representative watersheds 04/2005 (2005–2011).

References

Alcoforado MJ, Andrade H (2006) Nocturnal urban heat island in Lisbon (Portugal): main features and modelling attempts. Theor Appl Climatol 84:151–159. doi:10.1007/s00704-005-0152-1

Arnfield AJ (1982) An approach to the estimation of the surface radiative properties and radiation budgets of cities. Phys Geogr 3:97–122

Arnfield AJ (2003) Two decades of urban climate research: a review of turbulence, exchanges of energy and water, and the urban heat island. Int J Climatol 23(1):1–26. doi:10.1002/joc.859

Bejarán RA, Camilloni IA (2003) Objective method for classifying air masses: an application to the analysis of Buenos Aires (Argentina) urban heat island intensity. Theor Appl Climatol 74:93–103. doi:10.1007/s00704-002-0714-4

Bretz S, Akbari H, Rosenfeld A (1998) Practical issues for using solar-reflective materials to mitigate urban heat islands. Atmos Environ 32(1):95–101. doi:10.1016/S1352-2310(97)00182-9

Carfan AC, Nery JT, Stivari SM (2007) Dinâmica dos ventos e temperatura do ar em Maringá, no verão de 2004. Revista Eletrônica Geografar 2(1):01–21. www.ser.ufpr.br/geografar. In Portuguese

Chander G, Markham BL, Helder DL (2009) Summary of current radiometric calibration coefficients for Landsat MSS, TM, ETM+, and EO-1 ALI sensors. Remote Sens Environ 113:893–903

Cheval S, Dumitrescu A (2008) The July urban heat island of Bucharest as derived from modis images. Theor Appl Climatol 91(1–4):1–9. doi:10.1007/s00704-008-0019-3

Cheval S, Dumitrescu A, Bell A (2009) The urban heat island of Bucharest during the extreme high temperatures of July 2007. Theor Appl Climatol 97:391–401. doi:10.1007/s00704-008-0088-3

Chung U, Choi C, Yun JI (2004) Urbanization effect on the observed change in mean monthly temperatures between 1951–1980 and 1971–2000 in Korea. Clim Change 66:127–136. doi:10.1023/B:CLIM.0000043136.58100.ce

De Griend V, Owe M (1993) On the relationship between thermal emissivity and the normalized difference vegetation index for natural surfaces. Int J Remote Sens 14:1119–1131

Ezber Y, Sen OL, Kindap T, Karaca M (2007) Climatic effects of urbanization in Istanbul: a statistical and modeling analysis. Int J Climatol 27(5):667–679. doi:10.1002/joc.1420

Freitas ED, Rozoff CM, Cotton WR, Silva Dias PL (2007) Interactions of an urban heat island and sea breeze circulations during winter over the Metropolitan Area of São Paulo—Brazil. Bound-Layer Meteorol 122(1):43–65. doi:10.1007/s10546-006-9091-3

Fujibe F (2009) Detection of urban warming in recent temperature trends in Japan. International J Climatol 29(12):1811–1822. doi:10.1002/joc.1822

Gallo KP, Tarpley JD, Mcnab AL et al (1995) Assessment of urban heat islands: a satellite perspective. Atmos Res 37:37–43. doi:10.1016/0169-8095(94)00066-M

Giridharan R, Lau SSY, Ganesan S, Givoni B (2007) Urban design factors influencing heat island intensity in high-rise high-density environments of Hong Kong. Build Environ 42(10):3669–3684. doi:10.1016/j.buildenv.2006.09.01

Grimmond CSB (2006) Progress in measuring and observing the urban atmosphere. Theor Appl Climatol 84:3–22. doi:10.1007/s00704-005-0140-5

Grimmond CSB, Oke TR (1991) An evapotranspiration-interception model for urban areas. Water Resour Res 27(7):1739–1755

Grimmond CSB, Oke TR (2002) Turbulent heat fluxes in urban areas: observations and a local-scale urban meteorological parameterization scheme (LUMPS). J Appl Meteorol 41(7):792–810. doi:10.1175/1520-0450(2002)041

Hafner J, Kidder SQ (1999) Urban heat island modeling in conjunction with satellite-derived surface/soil parameters. J Appl Meteorol 38:448–465. doi:10.1175/1520-0450(1999)038<0448:UHIMIC>2.0.CO;2

Homar V, Ramis C, Romero R, Alonso S (2010) Recent trends in temperature and precipitation over the Balearic Islands (Spain). Clim Change 98:199–211. doi:10.1007/s10584-009-9664-5

Huete A, Didan K, Miura T, Rodriguez EP, Gao X, Ferreira LG (2002) Overview of the radiometric and biophysical performance of the MODIS vegetation indices. Remote Sens Environ 83:195–213. doi:10.1016/S0034-4257(02)00096-2

Imhoff ML, Zhang P, Wolfe RE, Bounoua L (2010) Remote sensing of the urban heat island effect across biomes in the continental USA. Remote Sens Environ 114:504–513. doi:10.1016/j.rse.2009.10.008

Iqbal M (1983) An Introduction to Solar Radiation. Academic Press, Toronto

Jiang J, Tian G (2010) Analysis of the impact of land use/land cover change on land surface temperature with remote sensing. Proc Environ Sci 2:571–575. doi:10.1016/j.proenv.2010.10.062

Johansson E (2006) Influence of urban geometry on outdoor thermal comfort in a hot dry climate: a study in Fez, Morocco. Build Environ 41:1326–1338

Kanda M (2006) Progress in the scale modeling of urban climate: review. Theor Appl Climatol 84:23–33. doi:10.1007/s00704-005-0141-4

Karam HA, Oliveira AP, Soares J (1996) Simulação numérica da CLP em Candiota através de um modelo de mesoescala. Workshop on Air Pollution and Acid Rain: The Candiota Program. In Portuguese

Karam HA, Pereira Filho AJ, Masson V, Noilhan J, Marques Filho EP (2010) Formulation of a tropical town energy budget (t-TEB) scheme. Theor Appl Climatol 101:109–120. doi:10.1007/s00704-009-0206-x

Kinouchi T, Yoshitani J (2001) Simulation of the urban heat island in Tokyo with future possible increases of anthropogenic heat, vegetation cover and water surface. Proceedings of the International Symposium on Environmental Hydraulics. 6p

Kolokotroni M, Giridharan R (2008) Urban heat island intensity in London: an investigation of the impact. Sol Energy 82:986–998. doi:10.1016/j.solener.2008.05.004

Kusaka H, Kondo H, Kikegawa Y, Kimura F (2001) A simple single-layer urban canopy model for atmospheric models: comparison with multi-layer and slab models. Bound-Layer Meteorol 101:329–358. doi:10.1023/A:1019207923078

Lemonsu A, Grimmond CSB, Masson V (2004) Modeling the surface energy balance of the core of an old mediterranean city: Marseille. J Appl Meteorol 43:312–327. doi:10.1175/1520-0450(2004)043<0312:MTSEBO>2.0.CO;2

Li Q, Zhang H, Liu X et al (2004) Urban heat island effect on annual mean temperature during the last 50 years in China. Theor Appl Climatol 79:165–174. doi:10.1007/s00704-004-0065-4

Lin W, Wang B, Li J, Wang X, Zeng L, Yang L, Lin H (2010) The impact of urbanization on the monthly averaged diurnal cycle in October 2004 in the Pearl River Delta region. Atmosfera 23(1):37–51

Lucena AJ, Rotunno Filho OC, França JRA, Peres LF (2010a) The study of the urban heat islands in the metropolitan region of Rio de Janeiro. The Meeting of the Americas (AGU), Foz do Iguaçu/PR, In Portuguese

Lucena AJ, Rotunno Filho OC, França, JRA, Peres LF (2010b) Aplicação da correção atmosférica para imagens de satélite Landsat-TM. XV Congresso Brasileiro de Meteorologia, In Portuguese

Lucena AJ, Correa EB, Rotunno Filho OC, Peres LF, França JRA, Justi da Silva, MGA (2011) Ilhas de calor e eventos de precipitação na região metropolitana do Rio de Janeiro (RMRJ). XIV World Water Congress e 10o SILUSBA, In Portuguese

Manley G (1958) On the frequency of snowfall in metropolitan England. Q J R Meteorol Soc 84:70–72. doi:10.1002/qj.49708435910

Marques Filho EP, Karam HA, Miranda AG, Franca JRA (2009) Rio de Janeiro's urban climate. Urban Climate News—Quarterly Newsletter of the International Association of Urban Climate (IAUC), issue no. 32, June, 5–9. http://www.urban-climate.org

Martilli A, Clappier A, Rotach MW (2002) An urban surface exchange parameterization for mesoscale models. Bound-Layer Meteorol 104:261–304. doi:10.1023/A:1016099921195

Masson V (2000) A physically-based scheme for the urban energy budget in atmospheric models. Bound-Layer Meteorol 94:357–397. doi:10.1023/A:1002463829265

Mather PM (ed) (1993) Geographical information handling—research and applications. Wiley, New York

Murphy DJ, Hall MH, Hall CAS, Heisler GM, Stehman SV, Anselmi-Molina C (2011) The relationship between land cover and the urban heat island in northeastern Puerto Rico. Int J Climatol 31 (8):1222–1239. doi:10.1002/joc.2145

Oke TR (1976) The distinction between canopy and boundary-layer heat islands. Atmosphere 14:268–277

Oke TR (1981) Canyon geometry and the nocturnal urban heat island: comparison of scale model and field observation. J Climatol 1:237–254. doi:10.1002/joc.3370010304

Oke TR (1982) The energetic basis of the urban heat island. Q J R Meteorol Soc 108:1–24. doi:10.1002/qj.49710845502

Oke TR (1987) Boundary layer climate, 2nd edn. Routledge, London

Oke TR (1997) Surface climate processes. In: Bailey WG, Oke TR, Rouse WR (eds) Surface climates of Canada. McGill-Queen's University Press, Montreal, pp 21–43

Oke TR, Maxwell GB (1967) Urban heat island dynamics in Montreal and Vancouver. Atmos Environ 9(2):191–200. doi:10.1016/0004-6981(75)90067-0

Oke TR, Johnson GT, Steyn DG, Watson ID (1991) Simulation of surface urban heat islands under 'ideal' conditions at night. Part 2: diagnosis of causation. Bound-Layer Meteorol 56:339–358. doi:10.1007/BF00119211

Oleson KW, Bonan GB, Feddemab J, Jackson T (2011) An examination of urban heat island characteristics in a global climate model. Int J Climatol 31(12):1848–1865. doi:10.1002/joc.2201

Oliveira AP, Bornstein RD, Soares J (2003) Annual and diurnal wind patterns in the city of São Paulo. Water Air Soil Pollut: Focus 3:3–15. doi:10.1023/A:1026090103764

Peres LF, DaCamara CC (2006) Improving two-temperature method retrievals based on a nonlinear optimization approach. IEEE Geosci Remote Sens Lett 3:232–236. doi:10.1109/LGRS.2005.862274

Peres LF, Sobrino JA, Libonati R, Jimenez-Munoz JC, DaCamara CC, Romaguera M (2008) Validation of a temperature emissivity separation hybrid method from airborne hyperspectral scanner data and ground measurements in the SEN2FLEX field campaign. Int J Remote Sens 28:1–18. doi:10.1080/01431160802036532

Peres LF, DaCamara CC, Trigo IF, Freitas SC (2010) Synergistic use of the two-temperature and split-window methods for land-surface temperature retrieval. Int J Remote Sens 31:4387–4409. doi:10.1080/01431160903260973

Pigeon G, Moscicki MA, Voogt JA, Masson V (2008) Simulation of fall and winter surface energy balance over a dense urban area using the TEB scheme. Meteorol Atmos Phys 102:159–172. doi:10.1007/s00703-008-0320-9

Pongracz R, Bartholy J, Dezso Z (2006) Remotely sensed thermal information applied to urban climate analysis. Adv Space Res 37:2191–2196. doi:10.1016/j.asr.2005.06.069

Qin Z, Karnieli A, Berliner P (2001) A mono-window algorithm for retrieving land surface temperature from Landsat TM data and its application to the Israel–Egypt border region. Int J Remote Sens 22(18):3719–3746

Rao PK (1972) Remote sensing of urban heat islands from an environmental satellite. Bull Am Meteorol Soc 53:647–648

Rizwan AM, Dennis LYC, Liu C (2008) A review on the generation, determination and mitigation of urban heat island. J Environ Sci 20:120–128. doi:10.1016/S1001-0742(08)60019-4

Rosa-Freitas MG, Tsouris P, Reis IC, Figueiredo MA, Magalhães M, Nascimento TFS, Honório NA (2010) Dengue and land cover heterogeneity in Rio de Janeiro. Oecologia Australis 14(3):641–667. doi:10.4257/oeco.2010.1403.04

Rosenzweig C, Solecki WD, Parshall L et al (2005) Characterizing the urban heat island in current and future climates in New Jersey. Environ Haz 6:51–62. doi:10.1016/j.hazards.2004.12.001

Roth M (2007) Review of urban climate research in (sub) tropical regions. Int J Climatol 27:1859–1873. doi:10.1002/joc.1591

Saaroni H, Ben-Dor E, Bitan A et al (2000) Spatial distribution and microscale characteristics of the urban heat island in Tel-Aviv, Israel. Land Urban Plan 48:1–18. doi:10.1016/S0169-2046(99)00075-4

Sobrino JA, Jiménez-Muñoz JC, Paolini L (2004) Land surface temperature retrieval from LANDSAT TM 5. Remote Sens Environ 90:434–440. doi:10.1016/j.rse.2004.02.003

Souza JD, Silva BB (2005) Correção atmosférica para temperatura da superfície obtida com imagem TM: Landsat 5. Rev Bras Geofis 23(4):349–358, In Portuguese

Stathopoulou M, Cartalis C (2007) Daytime urban heat islands from Landsat ETM+ and Corine land cover data: an application to major cities in Greece. Sol Energy 81:358–368. doi:10.1016/j.solener.2006.06.014

Streutker DR (2003) Satellite-measured growth of the urban heat island of Houston, Texas. Remote Sens Environ 85:282–289. doi:10.1016/S0034-4257(03)00007-5

Sun CY, Brazel AJ, Chow WTL, Hedquist BC, Prashad L (2009) Desert heat island study in winter by mobile transect and remote sensing techniques. Theor Appl Climatol 98:323–335. doi:10.1007/s00704-009-0120-2

Taha H (1997) Urban climates and heat islands: albedo, evapotranspiration, and anthropogenic heat. Energy Build 25:99–103. doi:10.1016/S0378-7788(96)00999-1

Van Weverberg K, De Ridder K, Van Rompaey A (2007) Modeling the contribution of the Brussels heat island to a long temperature time series. J Appl Meteorol Climatol 47:976–990. doi:10.1175/2007JAMC1482.1

Velazquez-Lozada A, Gonzalez JE, Winter A (2006) Urban Heat island effect analysis for San Juan, Puerto Rico. Atmos Environ 40:1731–1741. doi:10.1016/j.atmosenv.2005.09.074

Voogt JA (2002) Urban heat island, causes and consequences of global environmental change. Encycl Glob Environ Chang 3:660–666

Voogt JA, Oke TR (2003) Thermal remote sensing of urban climates. Remote Sens Environ 86:370–384. doi:10.1016/S0034-4257(03)00079-8

Vukovich FM, Dunn JW, Crissman BW (1976) A theoretical study of the St. Louis heat island: the wind and temperature distribution. J Appl Meteorol 15:417–440. doi:10.1175/1520-0450(1976)015<0417:ATSOTS>2.0.CO;2

Weng Q, Lub D, Schubring J (2004) Estimation of land surface temperature–vegetation abundance relationship for urban heat island studies. Remote Sens Environ 89:467–483. doi:10.1016/j.rse.2003.11.005

Wilks DS (2006) Statistical methods in the atmospheric sciences, 2nd edn. Academic, London

Yoshikado H (1992) Numerical study of the daytime urban effect and its interaction with the sea breeze. J Appl Meteorol 31:1146–1164

Yoshikado H (1994) Interaction of the sea breeze with urban heat islands of different sizes and locations. J Meteorol Soc Jpn 72:139–143

Yuan F, Bauer ME (2007) Comparison of impervious surface area and normalized difference vegetation index as indicators of surface urban heat island effects in Landsat imagery. Remote Sens Environ 106:375–386. doi:10.1016/j.rse.2006.09.003

Zha Y, Gao J, Ni S (2003) Use of normalized difference built-up index in automatically mapping urban areas from TM imagery. Int J Remote Sens 24:583–594. doi:10.1080/01431160304987

Zhang N, Gao Z, Wang X, Chen Y (2010) Modeling the impact of urbanization on the local and regional climate in Yangtze River Delta, China. Theor Appl Climatol 102(3-4):331–342. doi:10.1007/s00704-010-0263-1

Zhang Y, Odeh IOA, Han C (2009) Bi-temporal characterization of land surface temperature in relation to impervious surface area, NDVI and NDBI, using a sub-pixel image analysis. Int J Appl Earth Obs Geoinf 11:256–264. doi:10.1016/j.jag.2009.03.001